ACS OMEGA

http://pubs.acs.org/journal/acsodf

Article

Interlayer Coupling Induced Sharp Increase of the Curie Temperature in a Two-Dimensional MnSn Multilayer

Panjun Feng,[⊥] Xiaohui Zhang,[⊥] Shuo Zhang, Dapeng Liu, Miao Gao, Fengjie Ma, Xun-Wang Yan,* and Zhi-Yuan Xie*

Cite This: *ACS Omega* 2022, 7, 43316−43320

Read Online

ACCESS | Metrics & More | Article Recommendations

ABSTRACT: The MnSn monolayer synthesized recently is a novel two-dimensional ferromagnetic material with a hexagonal lattice, in which three Mn atoms come together to form a trimer, making it remarkably different from other magnetic two-dimensional materials. Most impressively, there occurs a sharp increase of the Curie temperature from 54 to 225 K when the number of layers increases from 1 to 3. However, no quantitative explanation has been reported in previous studies. Herein, by means of the first-principles calculation method and the Monte Carlo method, we demonstrate that strong interlayer ferromagnetic coupling plays an essential role in enhancing its critical temperature, which acts as a magnetic field to stabilize the ferromagnetism in MnSn multilayers. Our work not only explains the sharp increase of the Curie temperature of the MnSn film in experiments but also reveals that the interlayer coupling is a new routine to achieve high-temperature ferromagnetism in two-dimensional materials.

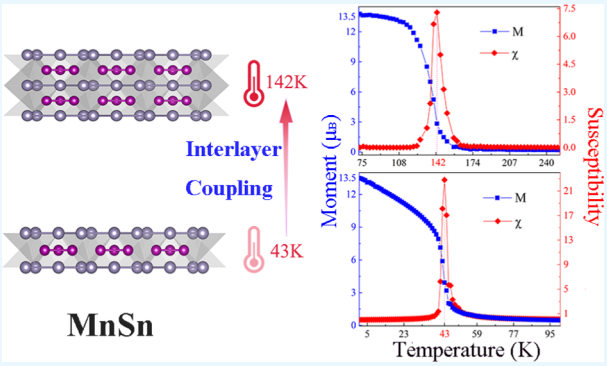

1. INTRODUCTION

The magnetic properties of two-dimensional materials have always been a hot topic in condensed matter physics and materials science fields. Graphene is the first two-dimensional material and possesses excellent mechanical properties, thermal conductivity, and electrical conductivity. However, nonmagnetism prevents graphene from application in the spintronics area. Thus, various means are used to realize the magnetism in graphene-related systems such as doping, chemical modification, defect, and boundary engineering. Unfortunately, such magnetic properties are disordered, nonintrinsic, and difficult to control. In 2016, Je-Geun Park proposed the concept of two-dimensional magnetic van der Waals materials.[1] In the same year, two-dimensional antiferromagnetic van der Waals materials $NiPS_3$ and $FePS_3$ were synthesized.[2,3] In 2017, two-dimensional ferromagnetic materials $Cr_2Ge_2Te_6$ and CrI_3 were discovered for the first time.[4,5] In 2018, room-temperature or near-room-temperature ferromagnetism of transition-metal dihalides VSe_2 and $MnSe_2$ was discovered.[6,7] Since then, the experimental and theoretical study of two-dimensional materials with intrinsic ferromagnetism has become a booming research field.[8−13]

For ferromagnetic two-dimensional materials synthesized experimentally, there are three main kinds of structures. The first one is the XY_3 structure represented by CrI_3, including $CrBr_3$, $CrCl_3$, VI_3, VBr_3, $FePS_3$, $MnPS_3$, $NiPS_3$, $Cr_2Ge_2Te_6$, $Cr_2Si_2Te_6$, and $CrCuP_2S_6$.[8,14] In these two-dimensional magnets, the core structure is an XY_3 octahedron, in which Y and X are at the apex and center of the octahedron, respectively, and each octahedron shares edges with the three surrounding octahedrons. The second typical structure is the XY_2 structure represented by VSe_2, including VS_2, $MnSe_2$, and NiI_2.[15] Its core structural unit is still an octahedron with a vertex of Y, but each octahedron shares edges with six surrounding octahedrons. The third structure is the XY structure, including FeTe and MnSe,[16] in which Y atoms form a tetrahedron and X is in the center of the tetrahedron. Thus, from the perspective of structure, the two-dimensional magnets synthesized in the experiment are mainly composed of octahedrons or tetrahedrons. Recently, the ferromagnetic MnSn monolayer and multilayer,[9] with the distinct structural features from the above materials, were fabricated by the molecular beam epitaxy growth method.

The atomic structure of the MnSn layer is from the experimental measurement.[9] The MnSn monolayer has a

Received: October 20, 2022
Accepted: November 7, 2022
Published: November 16, 2022

hexagonal lattice with the symmetry of the $P\bar{6}2m$ space group (No.189), and the lattice parameters are $a = b = 6.57$ Å. Each unit cell is composed of three Mn atoms and three Sn atoms. More interestingly, three Mn atoms are gathered together to form a trimer with an equilateral triangular shape, and Sn atoms make up a distorted kagome lattice. The top view of the MnSn monolayer is shown in Figure 1a. According to the

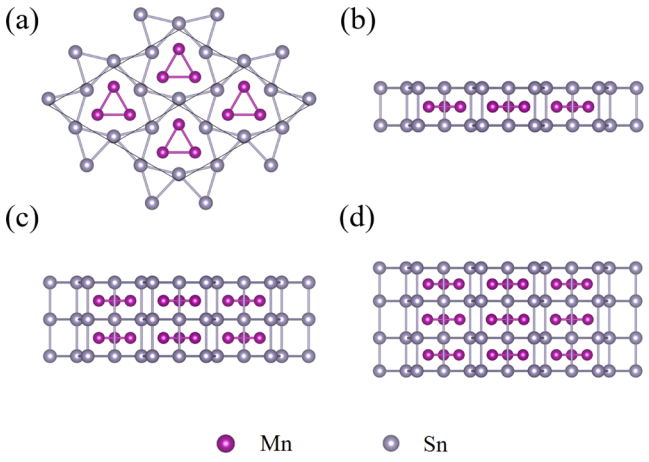

Figure 1. 2 × 2 unit cell of the MnSn monolayer, bilayer, and trilayer. (a) Top view; the unit cell is marked with a solid line rhombus. (b) Side view of the monolayer. (c) Side view of the bilayer. (d) Side view of the trilayer.

experimental samples reported in ref 9, the MnSn layer is synthesized on the Sn/Si buffer layer. Thus, we include a Sn buffer layer in our calculations to consider the influence of the buffer layer. The side views of the MnSn monolayer, bilayer, and trilayer on a Sn buffer layer are shown in Figure 1b–d, respectively. The Mn trimer and the distorted kagome lattice of Sn atoms are so unique that they do not appear in the reported crystal structures. These endow the MnSn material with particular electronic and magnetic properties. The most impressive feature is the sharp increase of the Curie temperature from 54, 225 to 235 K when the number of layers increases from 1, 3 to 4, and to date, no quantitative explanation has been reported.

In this study, by means of the first-principles calculation and Monte Carlo simulation method, we demonstrate that interlayer ferromagnetic coupling plays a significant role in realizing high-temperature ferromagnetism in the MnSn multilayer. In addition, we consider interlayer magnetic coupling as a magnetic field normal to the MnSn layer and enclose it into a two-dimensional Heisenberg model to evaluate the critical temperature, which provides a practical approach to estimate the critical temperature for multiple layers of magnetic materials.

2. COMPUTATIONAL METHOD

The calculations are carried out based on the plane-wave pseudopotential method enclosed in the VASP package, and the projector augmented-wave (PAW) pseudopotential with the Perdew–Burke–Ernzerhof (PBE) functional[17−20] is used. The GGA + U method is employed in our calculations because MnSn is a 3d transition-metal compound. The Hubbard U value of 5.66 eV is determined by the linear response approach developed by Matteo Cococcioni.[21] The plane-wave basis cutoff is 600 eV, and the convergence thresholds of total energy and force are 10^{-5} eV and 0.01 eV/Å, respectively. The vacuum layer is set to 20 Å to avoid interlayer interaction, and a mesh of 24 × 24 × 1 k-points is used to calculate the Brillouin zone integration for the primitive unit cell and a 12 × 12 × 1 k-point mesh is used for 2 × 2 supercells. The temperature of phase transition is evaluated by the Monte Carlo method, and the 100 × 100 lattice is used to represent the magnetic triangle lattice of the MnSn layer.[22]

3. RESULTS AND DISCUSSION

Figure 1 displays the 2 × 2 unit cell of the MnSn structure, including the top view (a) and side views for the monolayer (b), bilayer (c), and trilayer (d). In the MnSn layer, each Mn trimer acts as one lattice site and all sites make up a triangle lattice. We first investigate the magnetism of the MnSn monolayer. To find out the magnetic ground state, we calculate the energies of the MnSn monolayer with three magnetic orderings revealed by Figure 2. The energies are −39.026,

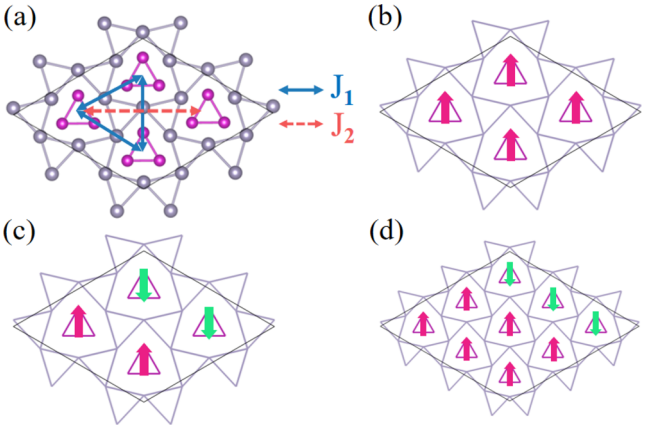

Figure 2. (a) Top view of the MnSn monolayer. J_1 and J_2 are the nearest and next-nearest neighboring magnetic interactions in the triangle lattice. (b) FM ordering, (c) AFM1 ordering, and (d) AFM2 ordering. The solid line rhombus represents the magnetic unit cell. To exhibit the magnetic orderings more clearly, the atomic structure is displayed with the wire frame.

−39.009, and −39.016 eV per unit cell for FM, AFM1, and AFM2 orderings, respectively, indicating that the MnSn monolayer on the Sn buffer layer exhibits a ferromagnetic behavior. The band structure of the MnSn monolayer in ferromagnetic ordering is presented in Figure 3a, in which multiple bands cross the Fermi level, indicating its metallic behavior. Figure 3b exhibits the projected density of states on Mn 3d orbitals and the Sn atom. The electronic states near the Fermi level are dominated by Sn atoms, while the spin polarization of Mn electrons makes a decisive contribution to the magnetization of the MnSn layer. As shown in Figure 3b, the spin-up states of five d orbitals are almost fully occupied and its spin-down states are empty, which results in the large local moment 4.7 μ_B.

To judge whether the ferromagnetic coupling of two adjacent MnSn layers is favorable or not, we calculate the energies of the MnSn bilayer and trilayer with different magnetic orders to estimate the interlayer magnetic interactions. For the MnSn bilayer, we chose a 1 × 2 × 2 supercell and display four magnetic orders from its side view, which are shown in Figure 4a–d, corresponding to FM′, AFM1′, AFM2′, and AFM3′, respectively. For AFM1′ and AFM2′ orderings

https://doi.org/10.1021/acsomega.2c06754
ACS Omega 2022, 7, 43316−43320

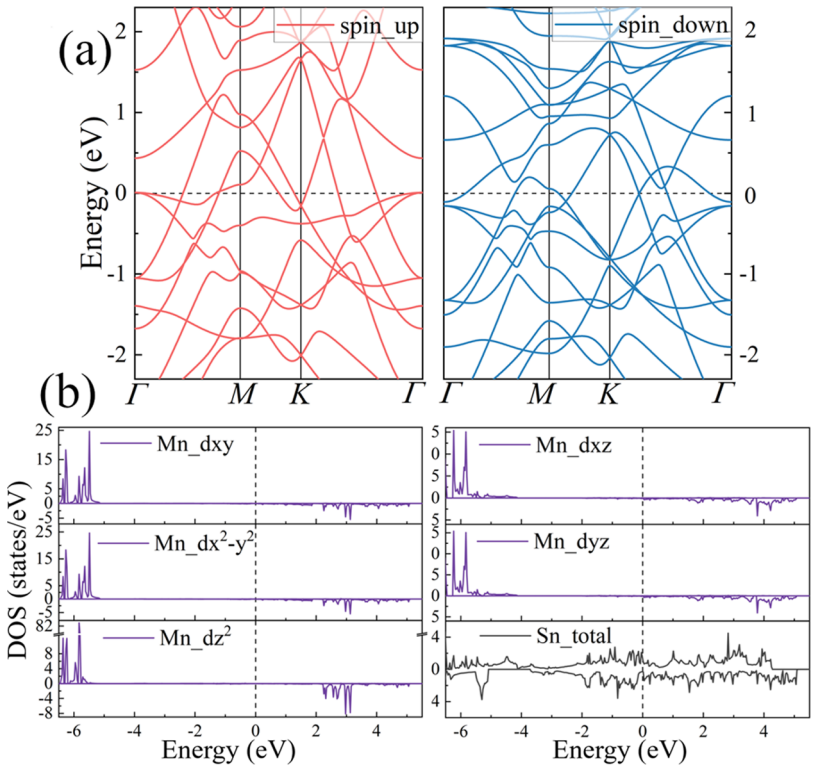

Figure 3. (a) Spin-up and spin-down band structures of the MnSn monolayer. (b) Projected density of states on Mn 3d orbitals and Sn atoms.

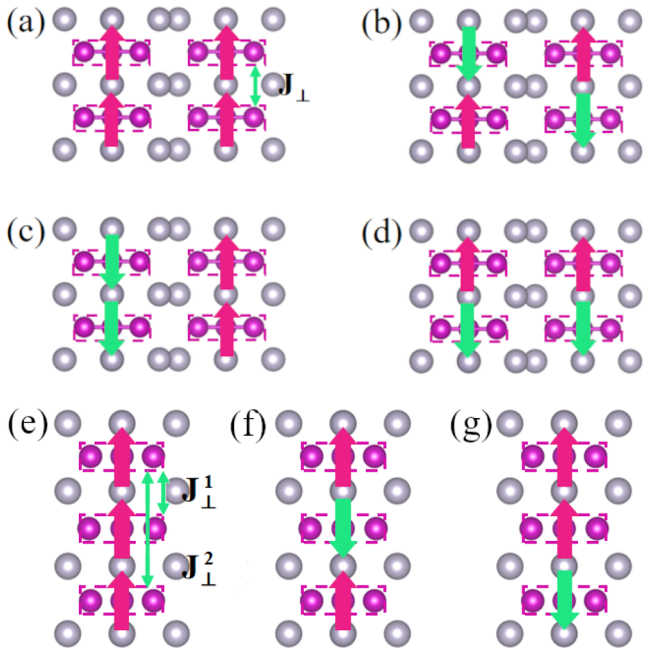

Figure 4. Side views of the 2 × 1 × 2 supercell and the 1 × 1 × 3 supercell. Red and green arrows indicate the directions of the magnetic moments on the Mn trimer. Four magnetic orders for the MnSn bilayer and three magnetic orders for the MnSn trilayer are shown in (a) FM′, (b) AFM1′, (c) AFM2′, (d) AFM3′, (e) FM″, (f) AFM1″, and (g) AFM2″, respectively. $J_{\perp}$, $J_{\perp}^{1}$, and $J_{\perp}^{2}$ are the interlayer magnetic couplings between two neighboring layers.

with the antiparallel moments in one layer, the energy of AFM2′ is lower than that of AFM1′, indicating that ferromagnetic interlayer coupling is preferred in the case of intralayer antiferromagnetism. For FM′ and AFM3′ orderings with parallel moments in one layer, the energy of FM′ is lower than that of AFM3′, indicating that ferromagnetic interlayer coupling is also preferred in the case of intralayer ferromagnetism. Thus, for the MnSn bilayer, the interlayer coupling is ferromagnetic. What about three layers? We build a 1 × 1 × 3 supercell composed of three MnSn layers to exhibit different interlayer magnetic couplings, and the related FM″, AFM1″, and AFM2″ are presented in Figure 4e−g, respectively. From AFM1″, AFM2″ to FM″, the energy goes down because of more ferromagnetic couplings. Therefore, this further demonstrates that the interlayer magnetic couplings are ferromagnetic for MnSn multilayers. In brief, the interlayer ferromagnetic coupling is confirmed by the calculations of the MnSn bilayer and the MnSn trilayer, which is in good agreement with the results in the experiments.[9]

Curie temperature is a vital parameter for ferromagnetic materials. At present, Curie temperature lower than room temperature is the main obstacle limiting the application of two-dimensional ferromagnetic materials in microscopic electronic devices. In our previous work,[11] we suggested that the dimerization of magnetic ions is an effective approach to realize high-temperature ferromagnetism. In the MnSn layer, three Mn ions form a trimer, and this leads to a large moment on one lattice site. Compared with a single Mn ion, the Mn trimer can obviously increase the magnetic interaction energy between two lattice sites. The critical temperature of magnetic phase transition is usually evaluated through solving the Heisenberg model with the Monte Carlo method.[23] For the two-dimensional Heisenberg model, the Hamiltonian is defined as

$$H = \sum_{<ij\alpha>} J_{1\alpha} S_{i\alpha} S_{j\alpha} + \sum_{\ll ij'\alpha\gg} J_{2\alpha} S_{i\alpha} S_{j'\alpha} + A \sum_{i} (S_{iz})^2 \quad (1)$$

https://doi.org/10.1021/acsomega.2c06754
ACS Omega 2022, 7, 43316−43320

in which the symbols j and j' represent the nearest and next-nearest neighboring sites of the i site in the triangle lattice, and α is the coordinate component x, y, or z. A is the single-site magnetic anisotropic energy. We perform the noncollinear magnetism calculations with the spin along the (1 0 0), (0 1 0), and (0 0 1) axis for different magnetic orderings, and the magnetic exchange interactions can be derived from these energies. There is no significant difference in the exchange interactions along different directions. For the MnSn monolayer, the exchange couplings are $J_{1x} = J_{1y} = J_{1z} = -5.46$ meV/S^2 and $J_{2x} = J_{2y} = J_{2z} = 1.34$ meV/S^2, and the single-site magnetic anisotropic energy is -0.636 meV/S^2 with the easy axis normal to the MnSn layer. The Curie temperature is 43 K, as reflected by the variation of the magnetic moment (M) and magnetic susceptibility ($\chi = \frac{<\vec{M}^2> - <\vec{M}>^2}{k_B T}$) with temperature in Figure 5a.

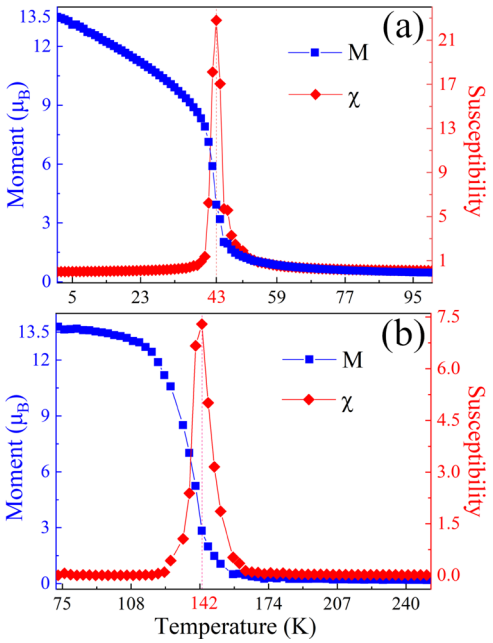

Figure 5. Average magnetic moment M and magnetic susceptibility χ as functions of temperature from the solution of the Heisenberg model on the triangle lattice for the MnSn monolayer (a) and bilayer (b).

As for the MnSn bilayer and multilayer, how to evaluate its Curie temperature on the basis of the results from electronic structure simulations is an interesting question. We chose one MnSn layer as our research object, in which the exchange couplings in the layer are computed, similar to the calculations of $J_{1\alpha}$ and $J_{2\alpha}$ in Expression 1. For this selected layer, the ferromagnetic interactions from its adjacent layer are considered effective magnetic fields normal to the MnSn layer, which can be derived from the energies of different magnetic orders. For the bilayer or multilayer system, the following Hamiltonian is used.

$$H = \sum_{<ij\alpha>} J_{1\alpha} S_{i\alpha} S_{j\alpha} + \sum_{\ll ij'\alpha\gg} J_{2\alpha} S_{i\alpha} S_{j'\alpha} + A \sum_i (S_{iz})^2 + \sum_i J_\perp (S_{\perp z} S_{iz}) \quad (2)$$

where the last term is the interlayer coupling. Apart from the last term, the Hamiltonian in Expression 2 is the same as in Expression 1. For the MnSn bilayer, the interlayer coupling $J_\perp$ is -84.16 meV/S^2. Compared to the exchange couplings of $J_{1x} = J_{1y} = J_{1z} = -5.46$ meV/S^2, the interlayer coupling $J_\perp$ of -84.16 meV/S^2 is a large value. It acts as a strong magnetic field on the MnSn layer, which forces the moments in a certain direction. The last term $\sum_i J_\perp (S_{\perp z} S_{iz})$ is regarded as $\sum_i H_{\text{eff}} \cdot S_{iz}$. Thus, the effective magnetic field is $H_{\text{eff}} = J_\perp S_{\perp z}$. By solving the Hamiltonian of the Heisenberg model in Expression 2 with the Monte Carlo method, the curve of magnetic phase transitions for the MnSn bilayer is obtained and is shown in Figure 5b. The Curie temperature of the MnSn bilayer is 142 K, much higher than the value of 43 K for the monolayer, which is because strong interlayer ferromagnetic interaction stabilizes its ferromagnetism. For the MnSn trilayer, the interlayer couplings $J_\perp^1$ and $J_\perp^2$ are -102.6 meV/S^2 and -4.7 meV/S^2, and the sum of $J_\perp^1$ and $J_\perp^2$ is $J_\perp = -107.3$ meV/S^2, higher than -84.16 meV/S^2 in the case of the bilayer. From the bilayer to the trilayer, the increase of interlayer coupling $J_\perp$ is due to the coupling from the third layer, which results in stronger ferromagnetism. From another point of view, the interlayer magnetic coupling is a new knob to adjust the ferromagnetism in two-dimensional materials, which provides another approach to enhance the Curie temperature of two-dimensional materials.

4. CONCLUSIONS

In summary, we systematically investigate the magnetic properties of the MnSn monolayer and the MnSn multilayers by means of the first-principles calculation and the Monte Carlo method. From the MnSn monolayer to the bilayer, the calculated Curie temperature varies from 43 to 142 K owing to the inclusion of strong ferromagnetic interactions between layers. Thus, we demonstrate that strong interlayer ferromagnetic coupling plays an essential role in enhancing its critical temperature, which acts as a magnetic field to stabilize the ferromagnetism in the MnSn multilayers. Our work not only explains the sharp increase of Curie temperature of the MnSn film from 54 to 225 K in experiments but also reveals that enhancing the interlayer coupling is a new routine to realize high-temperature ferromagnetism in two-dimensional materials.

AUTHOR INFORMATION

Corresponding Authors

Xun-Wang Yan − *College of Physics and Engineering, Qufu Normal University, Qufu, Shandong 273165, China*; orcid.org/0000-0001-8108-0791; Email: yanxunwang@163.com

Zhi-Yuan Xie − *Department of Physics, Renmin University of China, Beijing 100872, China*; Email: qingtaoxie@ruc.edu.cn

Authors

Panjun Feng − *College of Physics and Engineering, Qufu Normal University, Qufu, Shandong 273165, China*

Xiaohui Zhang − *Department of Physics, Renmin University of China, Beijing 100872, China*

Shuo Zhang − *College of Physics and Engineering, Qufu Normal University, Qufu, Shandong 273165, China*

Dapeng Liu − *College of Physics and Engineering, Qufu Normal University, Qufu, Shandong 273165, China*

https://doi.org/10.1021/acsomega.2c06754
ACS Omega 2022, 7, 43316−43320

Miao Gao − *Department of Physics, School of Physical Science and Technology, Ningbo University, Zhejiang 315211, China*
Fengjie Ma − *The Center for Advanced Quantum Studies and Department of Physics, Beijing Normal University, Beijing 100875, China*

Complete contact information is available at: https://pubs.acs.org/10.1021/acsomega.2c06754

Author Contributions

⊥P.F. and X.Z. contributed equally to this work.

Notes

The authors declare no competing financial interest.

■ ACKNOWLEDGMENTS

This work was supported by the National Natural Science Foundation of China (Grant Nos. 12274255, 11974207, 11974194, 11774420, and 12074040), the National R&D Program of China (Grant No. 2017YFA0302900), and the Major Basic Program of Natural Science Foundation of Shandong Province (Grant No. ZR2021ZD01).

■ REFERENCES

(1) Park, J.-G. Opportunities and challenges of 2D magnetic van der Waals materials: magnetic graphene? *J. Phys.: Condens. Matter* **2016**, *28*, No. 301001.
(2) Lee, J. U.; Lee, S.; Ryoo, J. H.; Kang, S.; Kim, T. Y.; Kim, P.; Park, C. H.; Park, J. G.; Cheong, H. Ising-Type Magnetic Ordering in Atomically Thin FePS3. *Nano Lett.* **2016**, *16*, 7433−7438.
(3) Kuo, C. T.; Neumann, M.; Balamurugan, K.; Park, H. J.; Kang, S.; Shiu, H. W.; Kang, J. H.; Hong, B. H.; Han, M.; Noh, T. W.; Park, J. G. Exfoliation and Raman Spectroscopic Fingerprint of Few-Layer NiPS 3 Van der Waals Crystals. *Sci. Rep.* **2016**, *6*, No. 20904.
(4) Gong, C.; Li, L.; Li, Z.; Ji, H.; Stern, A.; Xia, Y.; Cao, T.; Bao, W.; Wang, C.; Wang, Y.; Qiu, Z. Q.; Cava, R. J.; Louie, S. G.; Xia, J.; Zhang, X. Discovery of intrinsic ferromagnetism in two-dimensional van der Waals crystals. *Nature* **2017**, *546*, 265−269.
(5) Huang, B.; Clark, G.; Navarro-Moratalla, E.; Klein, D. R.; Cheng, R.; Seyler, K. L.; Zhong, D.; Schmidgall, E.; McGuire, M. A.; Cobden, D. H.; Yao, W.; Xiao, D.; Jarillo-Herrero, P.; Xu, X. Layer-dependent ferromagnetism in a van der Waals crystal down to the monolayer limit. *Nature* **2017**, *546*, 270−273.
(6) Bonilla, M.; Kolekar, S.; Ma, Y.; Diaz, H. C.; Kalappattil, V.; Das, R.; Eggers, T.; Gutierrez, H. R.; et al. Strong room-temperature ferromagnetism in VSe2 monolayers on van der Waals substrates. *Nat. Nanotechnol.* **2018**, *13*, 289−293.
(7) O'Hara, D. J.; Zhu, T.; Trout, A. H.; Ahmed, A. S.; Luo, Y. K.; Lee, C. H.; Brenner, M. R.; Rajan, S.; Gupta, J. A.; McComb, D. W.; Kawakami, R. K. Room Temperature Intrinsic Ferromagnetism in Epitaxial Manganese Selenide Films in the Monolayer Limit. *Nano Lett.* **2018**, *18*, 3125−3131.
(8) Gong, C.; Zhang, X. Two-dimensional magnetic crystals and emergent heterostructure devices. *Science* **2019**, *363*, No. eaav4450.
(9) Yuan, Q.-Q.; Guo, Z.; Shi, Z.-Q.; Zhao, H.; Jia, Z.-Y.; Wang, Q.; Sun, J.; Wu, D.; Li, S.-C. Ferromagnetic MnSn Monolayer Epitaxially Grown on Silicon Substrate. *Chin. Phys. Lett.* **2020**, *37*, No. 077502.
(10) Liu, D.; Zhang, S.; Gao, M.; Yan, X.-W.; Xie, Z. Y. Robust ferromagnetism in single-atom-thick ternary chromium carbonitride CrN_4C_2. *Appl. Phys. Lett.* **2021**, *118*, No. 223104.
(11) Feng, P.; Zhang, S.; Liu, D.; Gao, M.; Ma, F.; Yan, X.-W.; Xie, Z. Y. Achieving High-Temperature Ferromagnetism by Means of Magnetic Ion Dimerization in the Graphene-like $Mn_2N_6C_6$ Monolayer. *J. Phys. Chem. C* **2022**, *126*, 10139−10144.
(12) Liu, D.; Feng, P.; Gao, M.; Yan, X.-W. CoN_4C_2: Two-dimensional cobalt carbonitride with a flat-band feature. *Phys. Rev. B* **2021**, *103*, No. 155411.
(13) Liu, D.; Zhang, S.; Gao, M.; Yan, X.-W. Prediction of the two-dimensional cobalt carbonitride compounds CoN_4C_{10}, $Co_2N_8C_6$, and $Co_2N_6C_6$. *Phys. Rev. B* **2021**, *103*, No. 125407.
(14) Zhang, S.; Xu, R.; Luo, N.; Zou, X. Two-dimensional magnetic materials: structures, properties and external controls. *Nanoscale* **2021**, *13*, 1398−1424.
(15) Hossain, M.; Qin, B.; Li, B.; Duan, X. Synthesis, characterization, properties and applications of two-dimensional magnetic materials. *Nano Today* **2022**, *42*, No. 101338.
(16) Blei, M.; Lado, J. L.; Song, Q.; Dey, D.; Erten, O.; Pardo, V.; Comin, R.; Tongay, S.; Botana, A. S. Synthesis, engineering, and theory of 2D van der Waals magnets. *Appl. Phys. Rev.* **2021**, *8*, No. 021301.
(17) Kresse, G.; Furthmüller, J. Efficient iterative schemes for ab initio total-energy calculations using a plane-wave basis set. *Phys. Rev. B* **1996**, *54*, 11169−11186.
(18) Kresse, G.; Hafner, J. Ab initio molecular dynamics for liquid metals. *Phys. Rev. B* **1993**, *47*, 558−561.
(19) Perdew, J. P.; Burke, K.; Ernzerhof, M. Generalized Gradient Approximation Made Simple. *Phys. Rev. Lett.* **1996**, *77*, 3865−3868.
(20) Blöchl, P. E. Projector augmented-wave method. *Phys. Rev. B* **1994**, *50*, 17953−17979.
(21) Cococcioni, M.; de Gironcoli, S. Linear response approach to the calculation of the effective interaction parameters in the LDA + U method. *Phys. Rev. B* **2005**, *71*, No. 035105.
(22) Zhang, Y.; Wang, B.; Guo, Y.; Li, Q.; Wang, J. A universal framework for metropolis Monte Carlo simulation of magnetic Curie temperature. *Comput. Mater. Sci.* **2021**, *197*, No. 110638.
(23) Torelli, D.; Olsen, T. Calculating critical temperatures for ferromagnetic order in two-dimensional materials. *2D Mater.* **2019**, *6*, No. 015028.